Available online at www.sciencedirect.com

ScienceDirect

Procedia CIRP 31 (2015) 118 – 123

www.elsevier.com/locate/procedia

15th CIRP Conference on Modelling of Machining Operations

Effects of Sequential Cuts on Residual Stresses when Orthogonal Cutting Steel AISI 1045

Mohamed N.A. Nasr

Dept. of Mechanical Engineering, Faculty of Engineering, Alexandria University, Alshatby, Alexandria, 21544, Egypt
Dept. of Materials Science & Engineering, Egypt-Japan University of Science & Technology, New Borg El-Arab, Alexandria, 21934, Egypt

* Tel.: +20-3-591-5848; fax: +20-3-590-2715. *E-mail address:* m.nasr@alexu.edu.eg.

Abstract

Residual stresses (RS) play a critical role in controlling part performance. Even though their final state may not only depend on the final finishing path, a few articles could be found on the effects of sequential cuts on RS. The current study focuses on modelling the effects of sequential cuts on RS, using finite element modelling, when dry orthogonal cutting AISI 1045. Different process parameters (cutting forces, temperatures, stresses, shear angle and plastic strain) were also examined, in order to explain the RS findings. For model validation, orthogonal cutting tests were performed on a CNC lathe, and surface RS were measured using XRD.

Peer-review under responsibility of the International Scientific Committee of the "15th Conference on Modelling of Machining Operations

Keywords: Residual stress, Finite element method (FEM), Sequential cut, Turning, Steel.

1. Introduction

Surface integrity critically controls the performance of mechanical components in different aspects. It mainly affects their mechanical and fatigue strength as well as corrosion resistance, especially in highly stressed components [1,2]. Surface integrity mainly encompasses surface roughness, hardness, grain size, grain orientation and residual stresses. Machining-induced residual stresses (RS) are one of the most important surface integrity parameters; accordingly, they have gained very special attention over the past few decades. Finite element modelling (FEM) has been used as an effective tool in such investigations; a few examples could be found in [2-5].

Even though a single-pass machining process almost does not exist in real life, the majority of the available FEM literature assumed a stress-free workpiece to start with, when modelling the cutting process and predicting RS. This neglects the fact that the near-surface layer undergoes severe plastic deformation and heat generation during the very first cut, which typically results in RS generation. In other words, a second cut would not start with a stress-free state and, accordingly, would possibly end up by different RS state.

To the author's best of knowledge, the first attempt to examine the effects of sequential cuts on RS was made by Sasahara et al. [6]. The authors investigated (experimentally and numerically) such effects when orthogonal cutting 70%Cu-30%Zn brass. Surface tensile RS were generated after roughing conditions (uncut chip thickness = 0.25 mm), and turned to be compressive after finishing conditions (uncut chip thickness = 0.10 mm). Further finishing passes had either neutral or negative impact, by regenerating surface tensile RS.

Liu and Guo [7] reported a drop in surface tensile RS after the second cut, when machining stainless steel AISI 304. Based on the used cutting conditions, surface compressive RS were even reported in some cases. In a later publication by the same authors [8], a critical uncut chip thickness was identified as a critical parameter that would result in flipping surface tensile RS to compressive. Ee et al. [9] reported no change in the type of surface RS when machining AISI 1045 steel, where tensile RS were generated in all cases. However, the

Peer-review under responsibility of the International Scientific Committee of the "15th Conference on Modelling of Machining Operations
doi:10.1016/j.procir.2015.03.032

thickness of tensile layer was found to significantly drop after the second cut. On the other hand, Outeiro et al. [10] reported an increase in the magnitude of surface tensile RS, as well as an increase in the thickness of tensile layer with sequential cuts when orthogonal cutting stainless steel AISI 316L.

Schulze et al. [11] addressed the effects of sequential cuts in processes with multi-edged tools, using FEM, focusing on the broaching process of SAE 5120 alloy steel. In a recent study by Zhao et al. [12], the authors modelled the effects of sequential cuts when micro-cutting oxygen-free high-conductivity copper (OFHC), using the smoothed-particle hydrodynamic (SPH) technique. After the second cut, an increase in chip curling with a decrease in chip thickness and cutting force component were reported; however, the thrust component did not really change. In addition, surface RS were found to be less tensile and turned to be compressive in some cases. In an article by Pu et al. [13], a profound effect for sequential cuts on RS was reported when cryogenic machining Mg alloy AZ31B; and, the authors recommended the use of at least two cutting passes before extracting RS from a finite element (FE) model.

It is obvious from the available literature that not enough attention has been paid to the effects of sequential cuts on RS. Accordingly, the current work investigates such effects when orthogonal cutting AISI 1045 (170 HV) steel. Experimental machining tests were performed, where surface RS were measured using X-ray diffraction (XRD). Sequential cuts were modelled using FEM, where a plane strain FE model was built using the commercial software ABAQUS. The numerical results were then compared to the experimental ones.

2. Experimental Work

Dry orthogonal cutting tests were performed on steel AISI 1045 (170 HV) disks (130 mm in diameter and 4.2 mm wide), using a CNC lathe (Boehringer VDF-180); Fig. 1 shows the used configuration. Cemented carbide inserts (Sandvik TLG-4250L-4125) with zero rake angle and 11° flank angle were used. A cutting speed of 100 m/min along with two feed rates (0.07 mm/rev and 0.14 mm/rev) was used. A fresh insert was used for each test, and each test was performed twice. The tool edge radius (r_n) was measured to be 22 µm. After each run, the tool edge was examined using an optical microscope for signs of wear, and none were found. Also, no signs of built-up-edge were found. Cutting force components were measured using a Kistler 9121 dynamometer. Surface RS in the cutting (circumferential) direction (RS11) were measured at the end of each cut, using XRD and the $sin^2\psi$ method, with CrKα source and a spot size of 3 mm. Each cut was run for 8 – 10 revolutions. Scanning electron microscopy was used to check for phase transformation, and no signs were found. Chips were collected for thickness measurement, using a digital calliper.

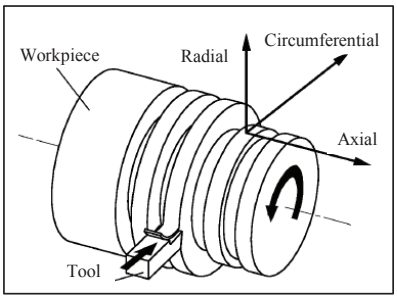

Fig. 1. Experimental cutting configuration (orthogonal conditions).

3. Finite Element Modelling (FEM)

3.1. General description and cutting conditions

Two-dimensional plane strain FE models were built, using the commercial software ABAQUS/Explicit, in order to simulate orthogonal dry cutting of AISI 1045 (170 HV) under the aforementioned experimental conditions. Simulations were run with zero rake angle, 11° flank angle, cutting velocity of 100 m/min, and uncut chip thickness (h); i.e., feed rate, of 0.07 mm and 0.14 mm. Coupled temperature-displacement analysis was used to account for temperature-dependent material properties, as well as heat generation and transfer.

3.2. Sequential cuts modelling

In the current work, only two cuts were considered to examine the effects of sequential cuts. This is also the typical procedure used in the literature [6-12], and supported by [13]. A Lagrangian model with two tools was built, shown in Fig. 2, where a delay time was implemented before the second tool starts cutting. The delay time represents the time taken by the disk to complete one full revolution, which was 0.25 seconds for the current conditions. The workpiece height was 1 mm for h = 0.07 mm and 1.5 mm for h = 0.14 mm, and the length was 3 mm. The workpiece bottom edge was totally fixed in space, and the velocity was applied to the tools. For the first cut, the workpiece initial temperature was 20 °C (room temperature). It is important to note that the two cuts had the same h value; either 0.07 mm or 0.14 mm. In other words, the target of the current work was not to investigate how roughing conditions would affect final RS. Rather, it was to investigate how two sequential identical passes would affect RS.

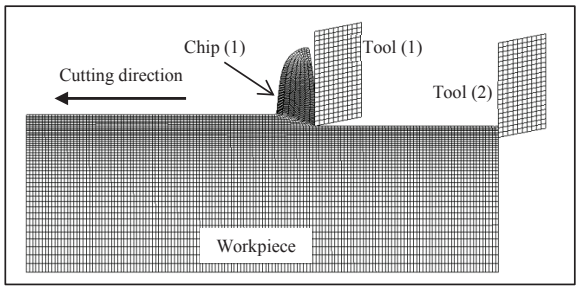

Fig. 2. Sequential cutting model (2 cuts).

3.3. Edge-radius (r_n) effects

In order to simulate the cutting process with non-sharp tools (i.e., take edge preparation effects into account), one of the following techniques need to be used; 1) Lagrangian formulation with a very fine mesh around the tool tip and continuous re-meshing [13]; 2) the arbitrary-Lagrangian-Eulerian (ALE) technique [2]; or, 3) the SPH technique [12]. To the author's best of knowledge, the first technique cannot be applied in ABAQUS; however, it is available in DEFORM, as an example [13]. At the same time, the SPH technique is still not well developed for modelling the cutting process, and using an ALE model for sequential cuts is not possible due to the change in size of different workpiece regions. More details about ALE partitioning and meshing schemes could be found in [2]. Accordingly, the only possible way to model sequential cuts in ABAQUS (current software) was to assume a sharp-edged tool and use the standard Lagrangian technique. In the current work, r_n was assumed to be 2 μm as a representation of sharp-edged tools.

Since there is no doubt that r_n plays an important role in the cutting process and RS generation [2,3,9], the following scenario was used in order to evaluate how the current assumption (r_n = 2 μm) would affect the results. First, an ALE model was built to simulate single pass cutting with the actual r_n value (22 μm), and the resulting RS were compared to those predicted by the Lagrangian model (r_n = 2 μm). This was done in order to isolate the effects of r_n on RS. The details of the used ALE model were first published in [2]. After that, the Lagrangian model with two tools (Fig. 2) was used to evaluate the effects of sequential cuts.

3.4. Residual stresses prediction

In order to predict RS, a relaxation simulation step is required (after the cutting step), where the workpiece is left to cool down to room temperature and the applied boundary conditions are deactivated. Accordingly, a relaxation step was required after each cut in order to evaluate the effects of sequential cuts on RS. It is worth mentioning that, for the second pass; first, an interim short cooling down step was simulated after the first run, before activating the second tool. The duration of the interim step is equal to the delay time (0.25 seconds) between the two cuts (Section 3.2). After the second cut, a full RS relaxation step was then run.

3.5. Constitutive model and chip generation

Temperature-dependant physical properties were assigned for the workpiece (AISI 1045), which were obtained from [14,15]. Plasticity was modelled using the well-known Johnson–Cook (J–C) model, with the values presented in Table 1 [16]. The melting and reference temperatures are 1480 ^{o}C and 20 ^{o}C, respectively. For chip separation, material failure was predicted based on the cumulative damage law using the well-known J-C failure model (shear failure). The AISI 1045 J-C damage parameters ($D_1 – D_5$) are presented in Table 2 [17].

Table 1. AISI 1045 J-C plasticity parameters [16].

A (MPa)	B (MPa)	n	C	$\dot{\varepsilon}_0$ (s^{-1})	m
553	600	0.234	0.0134	1	1

Table 2. AISI 1045 J-C cumulative damage parameters (unit-less) [17].

D_1	D_2	D_3	D_4	D_5
0.06	3.31	-1.96	0.0018	0.58

3.6. Heat generation and heat transfer

There are two sources of heat generation in metal cutting; friction and plastic deformation. Surface-to-surface contact pairs were used to define contacts between the tool and workpiece. The simple Coulomb friction model was used, and a friction coefficient of 0.2 was assumed. All frictional energy was assumed to be converted into heat. Based on the workpiece and tool properties, 37% of the generated heat was conducted into the tool. For plastic deformation, 90% of its energy was assumed to be converted into heat. During the cutting step, heat transfer to the surroundings (air) was neglected; however, it was defined in the relaxation step, with a convection coefficient of 10 W/(m^2 ^{o}C) [2] and a sink temperature of 20 ^{o}C. Heat radiation was neglected.

4. Results and Discussion

The effects of sequential cuts on RS, when orthogonal cutting AISI 1045, are presented below. In order to understand such effects, different process parameters were examined and compared to experimental results, when available. As mentioned earlier, XRD measurements were performed after 8 – 10 passes.

4.1. Residual stresses

Fig. 3 compares the predicted surface RS11 after the first and second cuts to XRD measurements. For the first cut, two cases are presented; r_n = 22 μm (ALE model) and r_n = 2 μm (Lagrangian model). The error bars represent the standard deviation of XRD measurements, which was also assumed to apply to FEM results for a fair comparison. It is worth mentioning that, the FEM results represent the average over a length of 200 μm (equivalent to 10 elements); however, XRD measurements represent the average over 3 mm (spot size).

As shown, surface tensile RS11 were generated in all cases; however, FEM underestimated their magnitudes, even when the actual r_n value (22 μm) was simulated. The sharp-edged tool (r_n = 2 μm) resulted in higher tensile RS, which agrees with the literature [2], yet lower than the experimental values. The second cut resulted in lower surface tensile RS, especially at higher h value. Therefore, a better prediction would not have been achieved even if the second cut were to be modelled using the ALE technique. Accordingly, the current underestimation is believed to be mainly attributed to the used material (from the literature) and friction (assumed) models, not to r_n. Therefore, the current findings would be still valid, at least qualitatively, regardless of the magnitude of r_n.

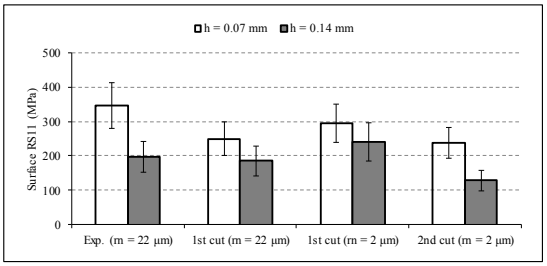

Fig. 3. Surface RS in cutting direction (RS11) – experimental (exp.) vs. FEM.

Focusing on the effects of sequential cuts, Fig. 4 presents the predicted in-depth RS11 profiles after the first and second cuts (r_n = 2 µm). As shown, the second cut resulted in less near-surface tensile stresses and a drop in the thickness of the tensile layer, especially for the larger h value. The current findings agree with the literature for different materials [6-9,12], and are explained in the following sections.

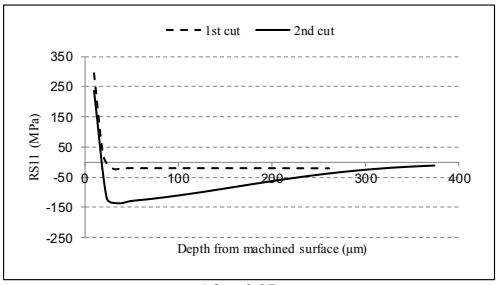

a) h = 0.07 mm

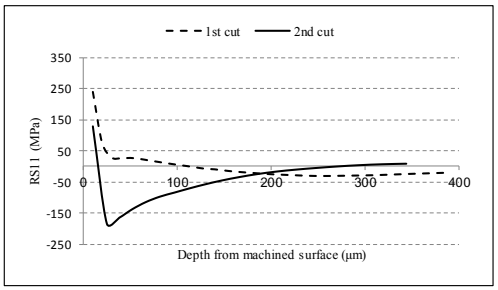

b) h = 0.14 mm

Fig. 4. In-depth RS distribution in cutting direction (RS11).

4.2. Cutting forces

Table 3 presents the measured and predicted cutting (F_c) and thrust (F_t) force components. With sequential cuts, a slight drop was noticed in F_c, similar to what was reported in [12]; such drop was more obvious at lower h value. The same behaviour was noticed with F_t. This could be attributed to the slightly higher temperatures during the second cut, as shown in Section 4.4, which results is thermal softening. For the examined range of r_n and h, r_n mainly affected F_t (where lower r_n resulted in lower F_t) but had almost no effect on F_c. As expected, such effect was more significant at lower h values. Compared to the measured forces, the predicted F_c was slightly lower; however, F_t was significantly underestimated even with r_n = 22 µm. The underestimation of F_t explains the drop in surface tensile RS, as it indicates that less material is plastically compressed underneath the tool tip [2].

Table 3. Cutting force components (values between quotations represent r_n).

h (mm)	Force component	Exp. (N/mm) "22 µm"	FEM (N/mm) 1st Cut "22 µm"	1st Cut "2 µm"	2nd Cut "2 µm"
0.07	F_c	190	181	188	175
	F_t	140	71	37	35
0.14	F_c	349	319	310	305
	F_t	256	102	66	60

4.3. Shear angle, CCR and tool-chip contact length

Table 4 presents the effects of sequential cuts on shear angle (φ), chip compression ratio (CCR) and tool-chip contact length (l_c), and compares them to experimental results. The experimental value of l_c was estimated based on that of CCR, as per Eq. 1 [18], which is valid for CCR < 4 as in the current case. φ was calculated using Eq. 2 [19], where γ is the rake angle. The current underestimation of l_c could be attributed to the used friction model which could not capture the stick-slip behaviour. It could be also partially attributed to r_n, as smaller r_n was found to result in slightly smaller φ and higher CCR when orthogonal cutting 0.2% carbon steel [20].

$$l_c = h*CCR^{1.5} \quad (1)$$

$$\tan(\varphi) = \frac{\cos(\gamma)}{CCR - \sin(\gamma)} \quad (2)$$

Table 4. Tool-chip contact length (l_c), CCR and shear angle (φ).

h (mm)	Parameter	Exp.	FEM (r_n = 2 µm) 1st Cut	2nd Cut
0.07	CCR	3	3.5	3.5
	l_c (mm)	0.363	0.217	0.217
	φ (°)	18.4	15.9	15.9
0.14	CCR	2.57	3	2.9
	l_c (mm)	0.577	0.322	0.322
	φ (°)	21.3	18.4	19.0

4.4. Workpiece temperatures

Fig. 5 shows the temperature distribution in the chip generation region for the two cuts, when h = 0.07 mm. The maximum temperature in the primary shear zone was 356 °C and 362 °C for the first and second cuts, respectively. The corresponding values for h = 0.14 mm were 354 °C and 374 °C, respectively. As shown, slightly higher temperatures were generated in the second cut, especially for h = 0.14 mm.

Fig. 6 presents the temperature distribution along the tool-chip contact length (l_c). For h = 0.07 mm, almost identical profiles were generated. On the other hand, for h = 0.14 mm, slightly higher temperatures were generated during the second cut; i.e., the effect of sequential cuts is more obvious at higher h values. This could be attributed to the increase in l_c with h (Table 4). Longer l_c means more friction, and subsequently, more heat generation and temperature rise along the rake face.

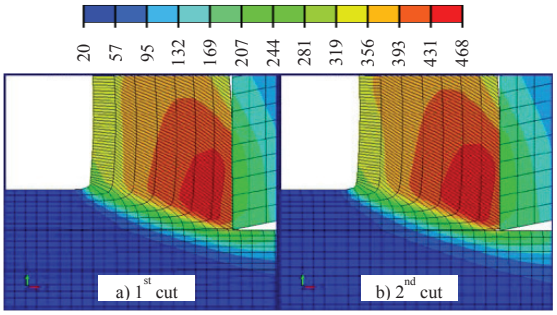

Fig. 5. Temperature distribution (°C) in chip formation zone (h = 0.07 mm).

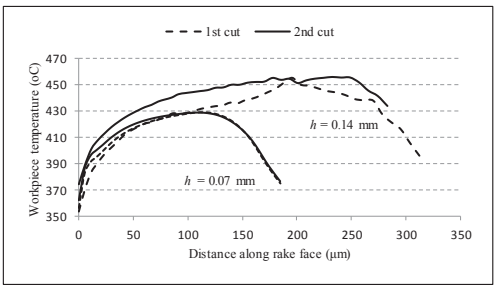

Fig. 6. Temperature distribution along the tool-chip contact length.

Checking the workpiece initial temperature before the second cut showed that the whole workpiece almost cooled down to room temperature when h = 0.07 mm. On the other hand, the average workpiece temperature for h = 0.14 mm was slightly higher (about 50 °C), with a temperature of 42 °C at the tool tip and a maximum of 58 °C, as shown in Fig. 7. This is attributed to the higher penetration depth of temperatures into the workpiece for h = 0.14 mm, as shown in Fig. 8, which is due to a slight increase in heat generation.

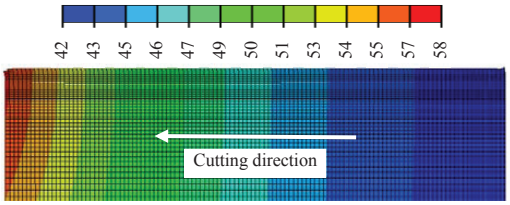

Fig. 7. Workpiece temperature (°C) at the beginning of 2nd cut (h = 0.14 mm).

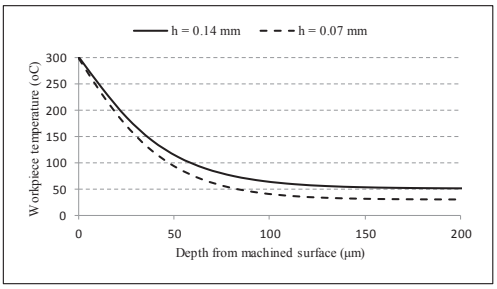

Fig. 8. Workpiece temperature underneath the tool tip during cutting (2nd cut).

4.5. Initial stress state

Fig. 9 presents the von Mises stress distribution underneath the tool tip during cutting. It is clear that, the second cut starts with an initial stress state that depends on h. Also, for both h values, slightly higher stresses were generated in the near-surface layer of the first cut. This could be attributed to the slightly lower temperatures generated in the first cut. After about 25-30 μm, sequential cuts had almost no effect on workpiece stresses. It is obvious that the depth of penetration of the generated stresses is much higher for h = 0.14 mm, which is mainly due to the increase in F_c with h.

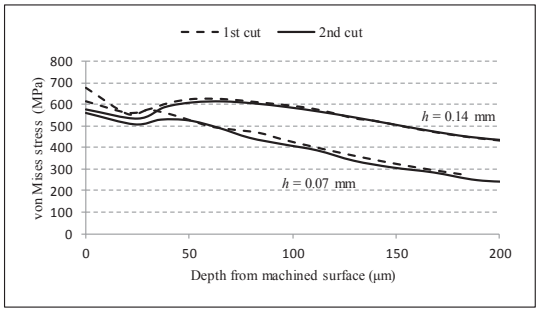

Fig. 9. Distribution of von Mises stress underneath the tool tip during cutting.

4.6. Plastic strain in cutting direction

Fig. 10 presents the distribution of plastic strain in cutting direction (PE11) in the machined surface, ahead of and behind the tool tip; note that the chip is not shown in the figure. As shown, the magnitude of compressive PE11 (ahead of the tool) is lower during the second cut. Since compressive PE11 results in tensile RS11 [4], this explains why lower surface tensile RS11 were generated in the second cut. At the same time, the drop in the magnitude of compressive PE11 between the two cuts is more significant when h = 0.14 mm, which explains the higher drop in surface tensile RS11 between the two cuts with higher h value.

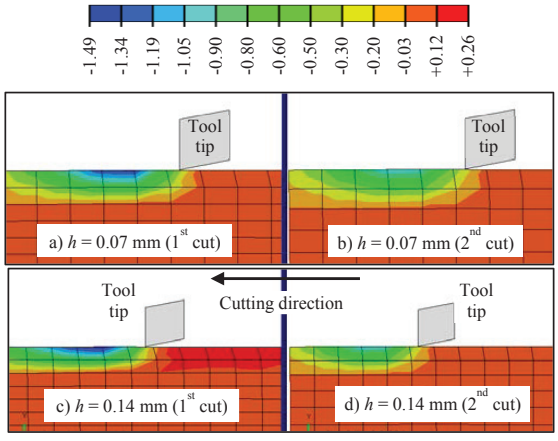

Fig. 10. Plastic strain in cutting direction (PE11) in machined surface (x 10^{-2}).

As mentioned above, compared to the second cut, the first cut experienced lower temperatures and higher stresses. Since: 1) for the same applied stress, lower strains are imposed with lower temperatures; and, 2) for the same temperature, higher strains are imposed with higher stresses; therefore, the higher compressive PE11 currently generated with lower *h* values means that the increase in stresses was more effective than the drop in temperatures. In other words, the initial stress state plays the major role (compared to initial temperatures) in controlling RS generated after sequential cuts.

5. Conclusions

The current study examined the effects of two sequential cuts on RS when orthogonal cutting AISI 1045, using two different uncut chip thicknesses (i.e., feed rates) at a constant speed. Based on the current results and presented discussion, the following conclusions were drawn.

1. Under the current conditions, surface tensile RS were generated in the cutting direction (RS11) in all cases.
2. The second cut resulted in lower surface tensile RS11, accompanied with a drop in the thickness of tensile layer; this was more obvious with larger uncut chip thickness.
3. Sequential cuts had almost no effect on shear angle, contact length, chip compression ratio. However, they resulted in slightly higher temperatures, lower stresses; i.e., lower cutting forces, and less compressive plastic strain in the cutting direction ahead of the tool tip. Again, such results were more significant with larger uncut chip thickness.
4. The current FE model underestimated RS, chip-tool contact length and the thrust force component (significantly). Such underestimated is believed to be mainly attributed to the used material model, as well as the friction model.
5. Sharp-edged tools resulted in higher surface RS11, and significantly lower thrust force component, but had a slight effect on the cutting force component.
6. It is believed that, the main reason for ending up with different RS distribution after the second cut is the initial stress state at the beginning of cutting (compared to a stress-free state for the first cut). Such effects are more significant when using a larger uncut chip thickness.

Acknowledgment

The author would like to thank Prof. M. Elbestawi, VP - Research & International Affairs, McMaster University, Canada, for facilitating the experimental work that was done at the McMaster Manufacturing Research Institute (MMRI) - Machining Science Lab (MSL).

References

[1] Jawahir IS, Brinksmeier E, M'Saoubi R, Aspinwall DK, Outeiro JC, Meyer D, Umbrello D, Jayal AD. Surface integrity in material removal processes: recent advances. CIRP Ann - Manuf Techn 2011; 60: 603-26.
[2] Nasr M, Ng EG, Elbestawi M. Modelling the effects of tool-edge radius on residual stresses when orthogonal cutting AISI-316L. Int J Mach Tool Manu 2007; 47: 401-11.
[3] Chen L, El-Wardany TI, Nasr M, Elbestawi M. Effects of edge preparation and feed when hard turning a hot work die steel with polycrystalline cubic boron nitride tools. CIRP Ann - Manuf Techn 2006; 55 (1): 89-92.
[4] Nasr M, Ng EG, Elbestawi M. Effects of strain hardening and initial yield strength on machining-induced residual stresses. J Eng Mater – T ASME 2007; 129: 567-79.
[5] Nasr M, Ng EG, Elbestawi M. Effects of workpiece thermal properties on machining-induced residual stresses – thermal softening & conductivity. J Eng Manuf - IMechE, part B, 2007; 221 (9): 1387-1400.
[6] Sasahara H, Obikawa T, Shirakashi T. FEM analysis of cutting sequence effect on mechanical characteristics in machined layer. J Mater Process Tech 1996; 62: 448-53.
[7] Liu CR, Guo YB. Finite element analysis of the effect of sequential cuts and tool-chip friction on residual stresses in a machined layer. Int J Mech Sci 2000; 42: 1069-86.
[8] Guo YB, Liu CR. FEM analysis of mechanical state on sequentially machined surfaces. Mach Sci Technol 2002; 6(1): 21–41.
[9] Ee KC, Dillon Jr. OW, Jawahir IS. Finite element modelling of residual stresses in machining induced by cutting using a tool with finite edge radius. Int J Mach Tool Manu 2005; 47: 1611-28.
[10] Outeiro JC, Umbrello D, M'Saoubi R. Experimental and FEM analysis of cutting sequence on residual stresses in machined layers of AISI 316L steel. Mater Sc Forum 2006; 524-525: 179-84.
[11] Schulze V, Osterried J, Strauß T. FE analysis on the influence of sequential cuts on component conditions for different machining strategies. Procedia Eng 2011; 19: 318-23.
[12] Zhao H, Liu C, Cui T, Tian Y, Shi C, Li J, Huang H. Influences of sequential cuts on micro-cutting process studied by smooth particle hydrodynamic (SPH). Appl Surf Sci 2013; 284: 366-71.
[13] Pu Z, Umbrello D, Dillon Jr. OW, Jawahir IS. Finite element simulation of residual stresses in cryogenic machining of AZ31B Mg alloy. Procedia CIRP 2014; 13: 282–87.
[14] ASM metals reference book. 2nd ed. Library of Congress; 1983.
[15] Yen YC, Söhner J, Lilly B, Altan T. Estimation of tool wear in orthogonal cutting using finite element analysis. J Mater Process Tech 2004; 146: 82-91.
[16] Jaspers SPFC, Dautzenberg JH. Material behaviour in metal cutting: strains, strain rates and temperatures in chip formation. J Mater Process Tech 2002; 121: 123-35.
[17] Duan CZ, Dou T, Cai YJ, Li YY. Finite element simulation and experiment of chip formation process during high speed machining of AISI 1045 steel. AMAE Int J Prod Ind Eng 2011; 2 (1): 28-32.
[18] Astakhov VP. Tribology of metal cutting. 1st ed. Oxford: Elsevier; 2006.
[19] Shaw MC. Metal Cutting Principles. 2nd ed. New York: Oxford University Press; 2005.
[20] Yen YC, Jain A, Altan T. A finite element analysis of orthogonal machining using different tool edge geometries. J Mater Process Tech 2004; 146: 72-81.